

---

# Learning Stochastic Behaviour of Aggregate Data

---

Shaojun Ma<sup>1</sup> Shu Liu<sup>1</sup> Hongyuan Zha<sup>2</sup> Haomin Zhou<sup>1</sup>

## Abstract

Learning nonlinear dynamics of aggregate data is a challenging problem since the full trajectory of each individual is not observable, namely, the individual observed at one time point may not be observed at next time point. One class of existing work investigate such dynamics by requiring complete longitudinal individual-level trajectories. However, in most of the practical applications, the requirement is unrealistic due to technical limitations, experimental costs and/or privacy issues. The other one class of methods learn the dynamics by regarding aggregate behaviour as a stochastic process with/without hidden variable. The performances of such methods may be restricted due to complex dynamics, high dimensions and computation costs. In this paper, we propose a new weak form based framework to study the hidden dynamics of aggregate data via Wasserstein generative adversarial network(WGAN) and Fokker Planck Equation(FPE). Our model fall into the second class of methods with simple structure and computation. We demonstrate our approach in the context of a series of synthetic and real-world datasets.

## 1. Introduction

**Trajectory data** is a kind of data that we are able to acquire the information of each individual all the time. Although sometimes the information of several individuals is missing, we still know how these individuals evolve and their correspondence at different time points. For example, stock price, weather, customer behaviors and most training datasets for computer vision and natural language processing. Unlike complete information of trajectory data, **aggregate data** is a kind of data that full trajectory of each individual is not available, meaning that there is no guaranteed individual level correspondence, some observed individuals at this time point may be unobserved at next time spot. In aggregate data, we care about the distribution of all individuals together and do not infer the exact information of each individual. For example, bird migration, DNA evolution and transport density.

In most realistic cases, collecting trajectory data is hard due to the privacy issues, technical limitations, time and monetary costs, etc. Aggregate data can be regarded as a random sampling of its according full trajectory data, for example, every time we observe a flock of birds, they are only a “subset” of the whole group and it is almost impossible for us to observe or identify a single bird twice, our goal in such a case is estimating the distribution of the birds flock at different time points.

There are several popular existing models to learn dynamics of aggregate data such as Hidden Markov Model (HMM)(Eddy, 1996), Kalman Filter (KF)(Harvey, 1990) and Particle Filter (PF) (Djuric et al., 2003). However, these models and their variants (Langford et al., 2009; Hefny et al., 2015) require full trajectories of each individual, which may not be available as we mentioned earlier. In the work of Hashimoto et al.(2016), a stochastic differential equation(SDE) was adopted to capture the dynamics of particles directly on observations, in which the drift coefficient is parameterized by a recurrent neural network. Furthermore, Wang et al.(2018) improved HMM by using a SDE to describe the evolving process of hidden states. It should be noted that though the work mentioned above and our method all treat drift coefficient as a neural network, our simpler objective function comes from a weak formulation view and can be naturally combined with WGAN(Arjovsky et al., 2017). We demonstrate the effectiveness of our model on different dimensional data.

Our method can also be regarded as a data-driven method of solving drift term in SDE and Fokker Planck Equation(FPE), where the latter is a special partial differential equation(PDE) that indicates density evolution. Without knowing analytical form of SDE and FPE, our model is capable of approximating the distribution of samples at different time points. Several methods of solving SDE and FPE (Weinan et al., 2017; Beck et al., 2018; Li et al., 2019) adopt opposite ways to our method, they utilize neural networks to estimate the real distribution  $P(x, t)$  with determined drift and diffusion terms. Additionally, in our model, though we treat diffusion term as a constant, it is also straightforward to treat it as a neural network as well, which can be an extension of our work. In conclusion, our contributions are:

- First, we propose a data-driven framework to recover

drift function of a SDE.

- Second, our model is a natural connection between WGAN and FPE with the help of weak formulation, we provide a novel way to study SDE by deep learning means.
- Finally, we empirically demonstrate the effectiveness of our framework for learning nonlinear dynamics from aggregate observations on both synthetic and real-world datasets.

To the best of our knowledge, none of the existing methods connect WGAN and FPE in a weak formulation to study the data-driven SDE.

## 2. Proposed Method

### 2.1. Problem Definition

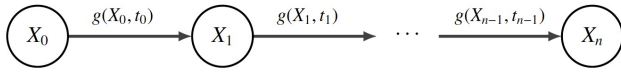


Figure 1. State model of the stochastic process  $X_t$

We assume the evolving process of individuals satisfies a SDE:

$$dX = g(X, t)dt + \sigma dW \quad (1)$$

this is an Itô process and we use its Euler increment form to give numerical approximation:

$$X_{t+\Delta t} = X_t + g(X_t, t)\Delta t + \sigma \sqrt{\Delta t}N(0, 1) \quad (2)$$

where the distribution of  $X_t$  represents the observation at time point  $t$ ,  $dX$  is the tiny change of  $x$  along with time interval  $dt$ ,  $g(x, t)$  is called drift term which drives the dynamics of the SDE,  $\sigma$  is the diffusion term,  $dW$  is a stochastic process and  $N(0, 1)$  is a standard Gaussian noise.

Our task can be described as: base on the assumption that the data evolves as a Itô process, given a series observations  $X_i$ , we aim to recover the drift coefficient  $g(x, t)$  by deep learning means. For simplicity we treat  $g(x, t)$  as a function uncorrelated to time  $t$ , namely,  $g(x, t) = g(x)$ .

### 2.2. Weak Form of Partial Differential Equation

In general, a PDE of the unknown function  $u(x_1, x_2, \dots, x_n)$  takes the form:

$$F(x, u, Du, u_{x_1x_1}, u_{x_1x_2}, \dots, u_{x_nx_n}, \dots) = 0 \quad (3)$$

where  $x = (x_1, x_2, \dots, x_n)$ ,  $Du = (u_{x_1}, u_{x_2}, \dots, u_{x_n})$ ,  $F$  is a function of the independent variable  $x$  and the unknown

function  $u$  and finitely many partial derivatives of  $u$ . The equation is called  $m$ -th order if the highest order of the derivatives of  $u$  in is  $m$ . We then multiply both sides of (3) by a test function  $f \in H_0^1(\Omega; \mathbb{R})$  and the integration on both sides leads to the weak formulation of (3):

$$\int_{\Omega} F(x, u, Du, u_{x_1x_1}, u_{x_1x_2}, \dots, u_{x_nx_n}, \dots)f(x) = 0 \quad (4)$$

where  $H_0^1(\Omega; \mathbb{R})$  denote the Sobolev space. If  $u \in H^1(\Omega; \mathbb{R})$  with possibly nonzero trace satisfies (3) for all  $f \in H_0^1$ , then we say  $u$  is a weak solution of (4). The first advantage of weak solution is that the strict solution of a PDE requires sufficient regularity of the problem thus may not exist in the classical sense, however the weak solution may exist and provide more advantages of solving PDEs(Zang et al., 2019). Another advantage is that by writing an integration form, we are able to investigate density in sample level so that machine learning methods could be applied.

### 2.3. Fokker Planck Equation

The density of a solution of SDE in Section 2.1 leads to an important partial differential equation: Fokker Planck Equation.

**Lemma 1.** Suppose  $\phi(x): \mathbb{R}^d \mapsto \mathbb{R}^n$  have a continuous partial time derivative and continuous second partial space derivatives, then the density of  $\phi$  that satisfies (1) leads to Fokker Planck Equation:

$$\frac{\partial P}{\partial t} = \sum_{i=1}^D -\frac{\partial}{\partial x_i} [g(x)P(x, t)] + \frac{1}{2}\sigma^2 \sum_{i,j=1}^D \frac{\partial^2}{\partial x_i \partial x_j} P(x, t)$$

As a linear evolution PDE, FPE describes the evolution of density functions of the stochastic process driven by a SDE. Due to this reason, FPE plays a crucial role in stochastic calculus, statistical physics and modeling (Nelson, 1985; Qi & Majda, 2016; Risken, 1989). Its importance is also getting more attention among statistic and machine learning community(Liu & Wang, 2016; Pavon et al., 2018; Rezende & Mohamed, 2015). In this paper, we utilize FPE to depict density evolution of the data, upon that we build our model by connecting FPE and deep learning methods through a weak formulation.

### 2.4. Weak Form of Wasserstein Distance

By Theorem 1, the probability density of observation  $x$ ,  $P(x, t)$ , satisfies Fokker Planck Equation:

$$\frac{\partial P}{\partial t} = \sum_{i=1}^D -\frac{\partial}{\partial x_i} [g(x, t)P(x, t)] + \frac{1}{2}\sigma^2 \sum_{i,j=1}^D \frac{\partial^2}{\partial x_i \partial x_j} P(x, t)$$

Suppose the observed samples at time points  $t_{m-1}$  and  $t_m$  are following  $\hat{P}(x, t_{m-1})$  and  $\hat{P}(x, t_m)$ , we utilize following

method to approximate distribution  $\tilde{P}(x, t_m)$ :

$$\tilde{P}(x, t_m) = \hat{P}(x, t_{m-1}) + \int_{t_{m-1}}^{t_m} \frac{\partial P(x, \tau)}{\partial \tau} d\tau \quad (5)$$

where  $x$  is the solution satisfies the SDE and  $P(x, \tau)$  is the true density of  $x$  at time  $\tau$ .

Then it is natural to compare the difference between two distributions  $\tilde{P}(x, t_m)$  and  $\hat{P}(x, t_m)$ . Applying Kantorovich-Rubinstein duality form(Villani, 2008), the Wasserstein distance between  $\tilde{P}$  and  $\hat{P}$  is:

$$W(\hat{P}, \tilde{P}) = \max_{\|\nabla f\| \leq 1} (\mathbb{E}_{X_r \sim \hat{P}(x, t_m)}[f(X_r)] - \mathbb{E}_{X_g \sim \tilde{P}(x, t_m)}[f(X_g)])$$

for some  $f$  whose gradient norm should be less or equal to 1. Notice that  $X_g$  is generated by  $g(x)$  from the initial data  $X_0$ , so above equation can be rewritten as a Wasserstein generative adversarial network (WGAN)(Arjovsky et al., 2017; Goodfellow et al., 2014) framework:

$$W(\hat{P}, \tilde{P}) = \max_{\|\nabla f\| \leq 1} (\mathbb{E}_{X_r \sim \hat{P}(x, t_m)}[f(X_r)] - \mathbb{E}_{X_0 \sim \tilde{P}(x, t_0)}[f(g(X_0))])$$

The way we deal with  $\mathbb{E}_{X_g \sim \tilde{P}(x, t_m)}[f(X_g)]$  is:

$$\begin{aligned} \mathbb{E}_{X_g \sim \tilde{P}(x, t_m)}[f(X_g)] &= \int_X f(x) \hat{P}(x, t_{m-1}) dx \\ &+ \int_X \int_{t_{m-1}}^{t_m} f(x) \frac{\partial P(x, \tau)}{\partial \tau} d\tau dx \end{aligned}$$

Then the second term on the right is actually a weak form of FPE and  $f(x)$  is the test function. This is the reason we call weak form of Wasserstein distance. We use integration by parts to deal with this term, refer the proof of Theorem 1 to see more details.

**Theorem 1.** Suppose  $f$  satisfies  $\|\nabla f\| \leq 1$  and generated data evolves only one step from  $x_{t_{m-1}}$  by (2), define an operator:

$$\begin{aligned} F(x_t) &= \frac{1}{N} \sum_{k=1}^N \left( \sum_{i=1}^D g(x_t^{(k)}) \frac{\partial}{\partial x_i} f(x_t^{(k)}) \right. \\ &\quad \left. + \frac{1}{2} \sigma^2 \sum_{i,j=1}^D \frac{\partial^2}{\partial x_i \partial x_j} f(x_t^{(k)}) \right) \end{aligned}$$

then the weak form of Wasserstein distance between real data and generated data at time point  $t_m$  can be approximated by:

$$\begin{aligned} \max_{\|\nabla f\| \leq 1} &\left( \frac{1}{N} \sum_{k=1}^N f(x_{t_m}^{(k)}) - \frac{1}{N} \sum_{k=1}^N f(x_{t_{m-1}}^{(k)}) \right. \\ &\quad \left. - \frac{\Delta t}{2} [F(x_{t_{m-1}}) + F(x_{t_m})] \right) \quad (6) \end{aligned}$$

By Theorem 1 we are able to compute the Wasserstein distance between two distributions on two consecutive time points. Different with normal form of Wasserstein distance, we have two extra terms at the end. This is because we consider time-series information that the data is following a dynamic density function, but not a static one as usual.

## 2.5. Wasserstein Distance on Time Series

The next question is that in real cases, it is not easy to observe the data on two consecutive time points, especially when  $\Delta t$  is really small. To make our model more flexible, we extend our result to followings so that we are able to deal with data on arbitrary time points.

**Theorem 2.** Suppose  $f$  satisfies  $\|\nabla f\| \leq 1$  and generated data evolves multiple steps from any initial data  $x_{t_{m_0}}$  by (2), define the operator:

$$\begin{aligned} F(x_t) &= \frac{1}{N} \sum_{k=1}^N \left( \sum_{i=1}^D g(x_t^{(k)}) \frac{\partial}{\partial x_i} f(x_t^{(k)}) \right. \\ &\quad \left. + \frac{1}{2} \sigma^2 \sum_{i,j=1}^D \frac{\partial^2}{\partial x_i \partial x_j} f(x_t^{(k)}) \right) \end{aligned}$$

then for arbitrary  $n$ , the weak form of Wasserstein distance between real data and generated data at time point  $t_m$  can be approximated by:

$$\begin{aligned} \max_{\|\nabla f\| \leq 1} &\left\{ \frac{1}{N} \sum_{k=1}^N f(x_{t_m}^{(k)}) - \frac{1}{N} \sum_{k=1}^N f(x_{t_{m_0}}^{(k)}) \right. \\ &\quad \left. - \frac{\Delta t}{2} (F(x_{t_{m_0}}) + F(x_{t_m}) + 2 \sum_{s=1}^{n-1} F(x_{t_{m_s}})) \right\} \quad (7) \end{aligned}$$

Finally we obtain objective function by minimizing the accumulated Wasserstein distance on time-series observations:

$$\begin{aligned} \min_g \sum_{n=1}^J \max_{f_n} &\left\{ \frac{1}{N} \sum_{k=1}^N f_n(x_{t_m}^{(k)}) - \frac{1}{N} \sum_{k=1}^N f_n(x_{t_{m_0}}^{(k)}) \right. \\ &\quad \left. - \frac{\Delta t}{2} (F(x_{t_{m_0}}) + F(x_{t_m}) + 2 \sum_{s=1}^{n-1} F(x_{t_{m_s}})) \right\} \quad (8) \end{aligned}$$

We call our algorithm Fokker Planck Process(FPP) which is shown in Algorithm 1.

## 3. Implicit Constraint of Drift Function

When dealing with realistic datasets, during training process we expect the predictions are not too far from the ground truth. To achieve that we propose to add some constraints on the drift function(neural network  $g$ ). Notice that put implicit constraints on drift term can be regarded as an improvement of our model and is a potential direction in the

---

**Algorithm 1** Fokker Planck Process Algorithm
 

---

**Require:** Initialize  $f_{\theta_n}, g_\omega$

- 1: **for** # training iterations **do**
- 2:     **for** k steps **do**
- 3:         **for** time  $t_{m_s}, t_{m_n}$  in  $[t_{m_0} : T]$  **do**
- 4:             Generate  $x_{t_{m_s}}^{(k)}, x_{t_{m_n}}^{(k)}$  by  $g_\omega$
- 5:             Sample real  $\{x_{t_{m_n}}^{(k)}\}$  from  $\mathbb{P}(X_{t_{m_n}})$
- 6:         **end for**
- 7:         For each  $f_n$  compute:
- 8:              $F_n = F(x_{t_{m_0}}) + F(x_{t_{m_n}}) + 2 \sum_{s=1}^{n-1} F(x_{t_{m_s}})$
- 9:             Update  $f_n$  by  $\nabla_\theta (\frac{1}{N} \sum_{k=1}^N f_n(x_{t_{m_n}}^{(k)}))$
- 10:              $-\frac{1}{N} \sum_{k=1}^N f_n(x_{t_{m_0}}^{(k)}) - \frac{\Delta t}{2} F_n$
- 11:         **end for**
- 12:         Update  $g_\omega$  by  $\nabla_\omega \sum_{f_n} (-\frac{\Delta t}{2} F_n)$
- 13:     **end for**

---

future work. Within the scope of this paper, we start with adding a distance regularizer to the loss function, then the generated data will be bounded by minimizing the distance regularizer.

**Theorem 3.** Denote the mean of real data as  $x_{mean}$ , suppose the real data and fake data are both bounded by a boundary function  $b(x) = 0$ , then the distance between data point  $x_i$  and  $b(x) = 0$  is approximated by:

$$dis(x_i, b(x)) \approx (1 - y) \|(x_i - x_{mean})\|_2 \quad (9)$$

where  $y$  is the solution of:

$$b(yx_i - yx_{mean}) = 0$$

if we assume real data evolves inside of a bounded elliptical area, then:

$$b(x) = \left\| \frac{x - x_{mean}}{\sigma} \right\|_2^2 - 1 = 0$$

the value of  $y$  would be:

$$y = \sqrt{\frac{1}{\left\| \frac{proj_\sigma \mathbf{x}}{\sigma} \right\|_2^2}} \quad (10)$$

where  $proj_\sigma \mathbf{x}$  is the projection of  $(\mathbf{x}_i - \mathbf{x}_{mean})$  on principal component  $\sigma$  of the ground truth.

The principal component of ground truth could be found by singular value decomposition(SVD). We expect to minimize the accumulated distance between each data point and the

boundary. Our new objective function turns out to be:

$$\min_g \sum_{n=1}^M \max_{f_n} \left\{ \frac{1}{N} \sum_{k=1}^N f_n(x_{t_{m_n}}^{(k)}) - \frac{1}{N} \sum_{k=1}^N f_n(x_{t_{m_0}}^{(k)}) - \frac{\Delta t}{2} (F(x_{t_{m_0}}) + F(x_{t_{m_n}}) + 2 \sum_{s=1}^{n-1} F(x_{t_{m_s}})) + \alpha \sum_{k=1}^N dist(x_{t_{m_n}}^{(k)}, b(x)) \right\} \quad (11)$$

The algorithm with implicit constraint on drift function is shown in Algorithm 2.

---

**Algorithm 2** Fokker Planck Process Algorithm with Implicit Constraint on Drift Function
 

---

**Require:** Initialize  $f_{\theta_n}, g_\omega$

- 1: **Do** SVD for training data
- 2: **Determine** Boundary function  $b(x)$  for training data
- 3: **for** # training iterations **do**
- 4:     **for** k steps **do**
- 5:         **for** time  $t_{m_s}, t_{m_n}$  in  $[t_{m_0} : T]$  **do**
- 6:             Generate  $x_{t_{m_s}}^{(k)}, x_{t_{m_n}}^{(k)}$  by  $g_\omega$
- 7:             Sample real  $\{x_{t_{m_n}}^{(k)}\}$  from  $\mathbb{P}(X_{t_{m_n}})$
- 8:             Compute  $S_n = \sum_{k=1}^N dist(x_{t_{m_n}}^{(k)}, b(x_{t_{m_n}}))$
- 9:         **end for**
- 10:         For each  $f_n$  compute:
- 11:              $F_n = F(x_{t_{m_0}}) + F(x_{t_{m_n}}) + 2 \sum_{s=1}^{n-1} F(x_{t_{m_s}})$
- 12:             Update  $f_n$  by  $\nabla_\theta (\frac{1}{N} \sum_{k=1}^N f_n(x_{t_{m_n}}^{(k)}))$
- 13:              $-\frac{1}{N} \sum_{k=1}^N f_n(x_{t_{m_0}}^{(k)}) - \frac{\Delta t}{2} F_n + \alpha S_n$
- 14:         **end for**
- 15:         Update  $g_\omega$  by  $\nabla_\omega \sum_{f_n} (-\frac{\Delta t}{2} F_n + \alpha S_n)$
- 16:     **end for**

---

## 4. Error Analysis

In this section, we provide an error analysis of our model. Suppose the ground truth of drift function is  $g_r(x)$ , the drift function that we learn from data is  $g_f(x)$ , then original Itô process, Euler evolve process and approximated evolve process are as follows:

$$dX = g(x)dt + \sigma dW$$

$$X_{t+\Delta t}^r = X_t^r + g_r(X_t^r)\Delta t + \sigma \sqrt{\Delta t} N^r(0, 1)$$

$$X_{t+\Delta t}^f = X_t^f + g_f(X_t^f)\Delta t + \sigma \sqrt{\Delta t} N^f(0, 1)$$

Estimating the error between original Itô process and its Euler form can be very complex, here we cite the conclusion from (Milstein & Tretyakov, 2013) and focus more on the error between original form and our model.

**Lemma 2.** *With the same initial  $X_{t_0}$ , if there is a global Lipschitz constant  $K$  which satisfies:*

$$|g(x, t) - g(y, t)| \leq K|x - y|$$

*then after  $n$  steps, the expectation error between Itô process  $X_{t_n}$  and Euler forward process  $X_{t_n}^r$  is:*

$$\mathbb{E}|X_{t_n} - X_{t_n}^r| \leq K(1 + E|X_0|^2)^{1/2} \Delta t$$

Lemma 2 illustrates that the expectation error between original Itô process and its Euler form is not related to total steps  $n$  but time step  $\Delta t$ .

**Theorem 4.** *With the same initial  $X_{t_0}$ , suppose the generalization error of neural network  $g(x)$  is  $\varepsilon$ , for some global Lipschitz constant  $K$ :*

$$|g(x) - g(y)| \leq K|x - y|$$

*the derivative of  $g(x)$  satisfies:*

$$\sup g'(x) = L$$

*then after  $n$  steps with step size  $\Delta t = T/n$ , the expectation error between Itô process  $X_{t_n}$  and approximated forward process  $X_{t_n}^f$  is bounded by:*

$$\mathbb{E}|X_{t_n} - X_{t_n}^f| \leq \frac{\varepsilon}{L}(e^{LT} - 1) + K(1 + E|X_0|^2)^{1/2} \Delta t \quad (12)$$

Theorem 4 implies that besides time step size  $\Delta t$ , our expectation error interacts with three factors, generalization error, supremum value of  $g'(x)$  and total time length. In our experiments, we find the best way to decrease the expectation error is reducing the value of  $L$  and  $n$ .

## 5. Experiments

In this section, we evaluate our model on various types of synthetic and realistic datasets.

**Baselines:** We compare our model with two recently proposed methods. One model(NN) learns dynamics directly from observations of aggregate data(Hashimoto et al., 2016). The other one model(LEGEND) learn dynamics with the help of setting hidden variables(Wang et al., 2018). The baselines in our experiments are two typical representatives that have state-of-the-art performance on learning aggregate data. Furthermore, our model study directly on observations and treat the evolving process of the data as a SDE, which is on the same track with NN. As mentioned before, NN trains its recurrent neural network via optimizing Sinkhorn distance(Cuturi, 2013), our model starts with a view of weak form of PDE, focuses more on WGAN framework and easier computation.

### 5.1. Synthetic Data

We first evaluate our model on three synthetic datasets generated using three artificial dynamics: **Synthetic-1**, **Synthetic-2** and **Synthetic-3**.

**Experiment Setup:** In all synthetic data experiments, we set both of the drift function  $g$  and the discriminator  $f$  as simple fully-connected networks. The  $g$  network has one hidden layer and the  $f$  network has three hidden layers. Each layer has 32 nodes for both  $g$  and  $f$ . The only one activation function we choose is Tanh. Notice that since we need to calculate  $\frac{\partial^2 f}{\partial x^2}$ , the activation function of  $f$  must be twice differentiable to avoid weight gradient loss. In terms of training process of  $g$  and  $f$  we use the Adam optimizer (Kingma & Ba, 2014) with learning rate  $10^{-4}$ . Furthermore, we use spectral normalization to realize  $\|\nabla f\| \leq 1$  (Miyato et al., 2018). We initialize the weights with Xavier initialization (Glorot & Bengio, 2010) and train our model by Algorithm 1.

#### Synthetic-1:

$$x_0 \sim N(0, \Sigma_0)$$

$$x_{t+\Delta t}^f = x_t^f - (A^T x_t^f + B)\Delta t + \sigma \sqrt{\Delta t} N(0, 1)$$

#### Synthetic-2 and 3:

$$x_0 \sim N(0, \Sigma_0)$$

$$x_{t+\Delta t}^f = x_t^f - G x_t^f \Delta t + \sigma \sqrt{\Delta t} N(0, 1)$$

Here we need to further state more information about  $G$ :

$$G = \begin{bmatrix} \frac{1}{\sigma_1} \frac{N_1}{N_1+N_2} (x_1 - \mu_{11}) + \frac{1}{\sigma_2} \frac{N_2}{N_1+N_2} (x_1 - \mu_{21}) \\ \frac{1}{\sigma_1} \frac{N_1}{N_1+N_2} (x_2 - \mu_{12}) + \frac{1}{\sigma_2} \frac{N_2}{N_1+N_2} (x_1 - \mu_{22}) \end{bmatrix}$$

$$N_1 = \frac{1}{\sqrt{2\pi}\sigma_1} \exp\left(-\frac{(x_1 - \mu_{11})^2}{2\sigma_1^2} - \frac{(x_1 - \mu_{12})^2}{2\sigma_1^2}\right)$$

$$N_2 = \frac{1}{\sqrt{2\pi}\sigma_2} \exp\left(-\frac{(x_2 - \mu_{21})^2}{2\sigma_2^2} - \frac{(x_2 - \mu_{22})^2}{2\sigma_2^2}\right)$$

In Synthetic-1, this is two dimensional data following simple linear dynamics, where  $A = [4, 1]$ ,  $B = [-3, -3]$ . We let  $\Delta t = 0.01$ ,  $\sigma = 1$ ,  $\Sigma_0 = [(1, 0), (0, 1)]$ . The data size  $N=2000$ , we utilize true  $x_0$ ,  $x_{20}$  and  $x_{200}$ , sample 1200 data points from each of these three time points as the training set and treat the other 800 data points of each time point as the test set. We predict the distributions of  $x_{50}$  and  $x_{500}$  of the test set. In Synthetic-2, this is two dimensional data following complex nonlinear dynamics. We let  $\Delta t = 0.01$ ,  $\sigma = 1$ ,  $\Sigma_1 = \Sigma_2 = [(1, 0), (0, 1)]$ ,  $\mu_1 = [15, 15]$  and  $\mu_2 = [-15, -15]$ . By editing Synthetic-2 from a balanced version to a biased version, we obtain Synthetic-3, where  $\Delta t = 0.02$ ,  $\sigma = 1$ ,  $\Sigma_1 = [(1, 0), (0, 1)]$ ,  $\Sigma_2 = [(0.95, 0), (0, 0.95)]$ ,  $\mu_1 = [16, 12]$  and  $\mu_2 = [-18, -10]$ . With the same data size,

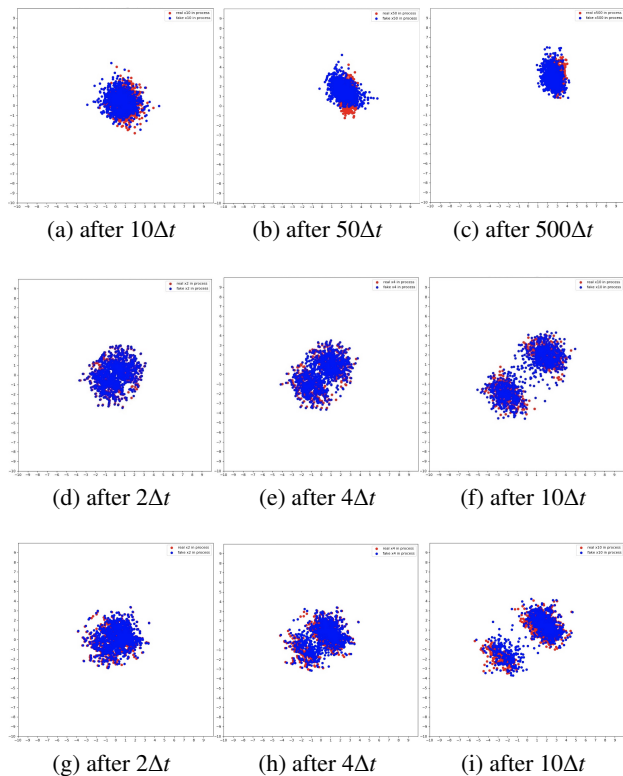


Figure 2. Comparison of generated data(blue) and ground truth(red) of Synthetic-1((a) to (c)), Synthetic-2((d) to (f)) and Synthetic-3((g) to (i)).

training set size and test set size, we utilize true  $x_0$ ,  $x_3$  and  $x_6$  as training set, predict the distributions of  $x_2$ ,  $x_4$  and  $x_{10}$  of the test set. We consider population evolution with three different dimensions:  $d = 2$ ,  $d = 6$  and  $d = 10$ . In each high dimensional case ( $d = 6$ ,  $d = 10$ ), to be convenience, we set every two dimensions follow the corresponding dynamics of low dimensional case( $d = 2$ ).

**Results:** We first show the capability of our model for learning hidden dynamics of low-dimensional ( $d = 2$ ) data. As visualized in Figure 2, the generated data(blue) almost covers all areas of ground truth(red), which demonstrates that our model is able to precisely learn the dynamics and correctly predict the future distribution of data. We then evaluate three models using Wasserstein distance as error metric for both low-dimensional ( $d = 2$ ) and high-dimensional ( $d = 6$ ,  $10$ ) data. As reported in Table 1, our model achieves lower Wasserstein error than the two baseline models in all cases. Additionally, with simpler structure, the training process of our model is easier without much computation time(as shown in Figure 3 (a) and (b)).

## 5.2. Realistic Data – RNA Sequence of Single Cell

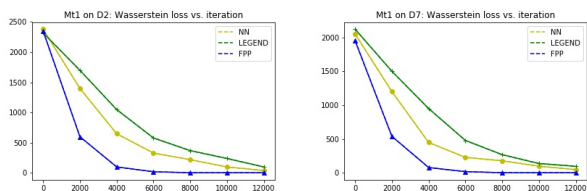
In this section, we evaluate our model on a biology dataset called Single-cell RNA-seq which is typically used for learn-

Table 1. The Wasserstein error of different models on Synthetic-1/2/3 and RNA-sequence datasets.

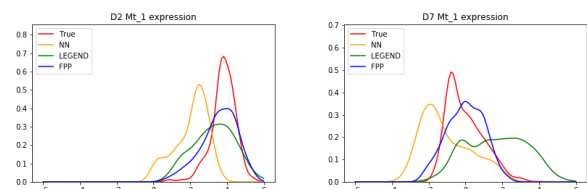
Data	Task	Dimension	NN	LEGEND	Ours
Syn-1	$x_{50}$	2	1.37	0.44	<b>0.05</b>
		6	4.79	2.32	<b>0.06</b>
		10	9.13	2.89	<b>0.10</b>
	$x_{500}$	2	0.84	0.18	<b>0.03</b>
		6	3.28	0.30	<b>0.03</b>
		10	8.05	1.79	<b>0.09</b>
Syn-2	$x_4$	2	5.53	1.27	<b>0.05</b>
		6	9.97	4.20	<b>0.08</b>
		10	16.51	6.08	<b>0.12</b>
	$x_{10}$	2	1.68	0.53	<b>0.05</b>
		6	4.84	1.08	<b>0.07</b>
		10	9.23	2.85	<b>0.11</b>
Syn-3	$x_4$	2	4.13	1.29	<b>0.08</b>
		6	6.40	3.16	<b>0.17</b>
		10	11.76	8.53	<b>0.25</b>
	$x_{10}$	2	3.05	0.87	<b>0.12</b>
		6	6.72	1.52	<b>0.16</b>
		10	9.81	3.55	<b>0.23</b>
RNA-Mt1	D2	10	33.86	10.28	<b>4.23</b>
	D7	10	12.69	7.21	<b>2.92</b>
RNA-Mt2	D2	10	31.45	13.32	<b>4.04</b>
	D7	10	11.58	7.89	<b>1.50</b>

ing the diffusion process where embryonic stem cells differentiate into mature cells (Klein et al., 2015). The cell population begins to differentiate from embryonic stem cells after the removal of LIF (leukemia inhibitory factor) at day 0 (D0). Single-cell RNA-seq observations are sampled at day 0 (D0), day 2 (D2), day 4 (D4) and day 7 (D7). At each time point, the expression of 24,175 genes of several hundreds cells are measured (933, 303, 683 and 798 cells on D0, D2, D4 and D7 respectively). We focus on the data of cell differentiation for the two chosen makers, i.e., Mt1 and Mt2. In first task we treat gene expression level at D0, D4 and D7 as training data to learn the hiding drift function and predict gene expression level at D2. In second task we train the model by gene expression level at D0, D2 and D4 to predict gene expression level at D7.

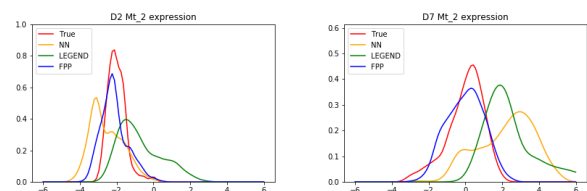
**Experiment Setup:** In realistic dataset, we set both  $f$  and  $g$  as fully connected three-hidden-layers neural networks, each layer has 64 nodes. The only activation function we choose is Tanh. The other setups of neural networks and training process are almost the same with the ones we use in Synthetic data, except that we train our model by Algorithm 2. Notice that in realistic case,  $\Delta t$  and  $T/\Delta t$  become hyperparameters, here we choose  $\Delta t = 0.05$ ,  $T/\Delta t = 30$ , which means the data evolves  $10\Delta t$  from D0 to D2, then  $10\Delta t$  from D2 to D4 and finally  $15\Delta t$  from D4 to D7. For preprocessing, we apply standard normalization procedures



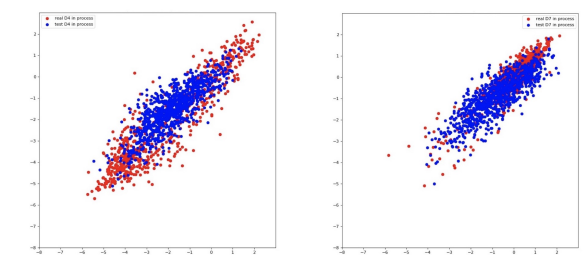
(a) Wasserstein loss of Mt1, D2 (b) Wasserstein loss of Mt1, D7



(c) Comparison on D2 of Mt1 (d) Comparison on D7 of Mt1



(e) Comparison on D2 of Mt2 (f) Comparison on D7 of Mt2



(g) Correlation comparison on D2

(h) Correlation comparison on D7

Figure 3. (a) and (b): Wasserstein loss as iteration increases of Mt1. (c) to (f): the performance comparison among different models on D2 and D7 of Mt1 and Mt2. (g) and (h): true (red) and predicted (blue) correlations between Mt1(x-axis) and Mt2(y-axis) on D2 (left) and D7 (right).

(Hicks et al., 2015) to correct batch effects and use non-negative matrix factorization to impute missing expression levels (Hashimoto et al., 2016; Wang et al., 2018).

**Results:** As shown in Table 1, when compared to other baselines, our model achieves lower Wasserstein error on both Mt1 and Mt2 data, which proves that our model is capable of learning the hidden drift term that governs dynamics and the evolve process of the two studied gene expressions. In Figure 3 (c) to (f), we visualized the predicted distributions of the two genes. When compared to the baseline models, the distributions of Mt1 and Mt2 predicted by our model

(curves in blue) are closer to the true distributions (curves in red) on both D2 and D7. Furthermore, our model precisely indicates the correlations between Mt1 and Mt2, as shown in Figure 3 (g) and (h), which also demonstrates the effectiveness of our model since closer to the true correlation represents better performance.

## 6. Conclusion

In this paper, we formulate a novel data-driven model to learn the drift term in a SDE. In particular, our work shows one can model aggregate observations as an Itô process and derives a new framework that employs Fokker Planck Equation with WGAN in a weak formulation. We also establish theoretical guarantees on the error estimation of our model. Finally we demonstrate through multiple synthetic datasets and a real Single-cell RNA-sequence dataset that our model performs well in different dimensional settings.

## References

- Arjovsky, M., Chintala, S., and Bottou, L. Wasserstein gan. In *arXiv preprint arXiv:1701.07875*, 2017.
- Beck, C., Becker, S., Grohs, P., Jaafari, N., and Jentzen, A. Solving stochastic differential equations and kolmogorov equations by means of deep learning. 2018.
- Cuturi, M. Sinkhorn distances: Lightspeed computation of optimal transport. In *Advances in Neural Information Processing Systems*, 2013.
- Djuric, P. M., Kotecha, J. H., Zhang, J., Huang, Y., Ghirmai, T., Bugallo, M. F., and Miguez, J. Particle filtering. *IEEE Signal Processing Magazine*, 20(5):19–38, 2003.
- Eddy, S. R. Hidden markov models. *Current Opinion in Structural Biology*, 6(3):361–365, 1996.
- Glorot, X. and Bengio, Y. Understanding the difficulty of training deep feedforward neural networks. In *International Conference on Artificial Intelligence and Statistics*, 2010.
- Goodfellow, I., Pouget-Abadie, J., Mirza, M., Xu, B., Warde-Farley, D., Ozair, S., Courville, A., and Bengio, Y. Generative adversarial nets. In *Neural Information Processing Systems*, 2014.
- Harvey, A. C. *Forecasting, structural time series models and the Kalman filter*. Cambridge University Press, 1990.
- Hashimoto, T., Gifford, D., and Jaakkola, T. Learning population-level diffusions with generative rnns. In *International Conference on Machine Learning*, pp. 2417–2426, 2016.

- Hefny, A., Downey, C., and Gordon, G. J. Supervised learning for dynamical system learning. In *Neural Information Processing Systems*, 2015.
- Hicks, S. C., Teng, M., and Irizarry, R. A. On the widespread and critical impact of systematic bias and batch effects in single-cell rna-seq data. *bioRxiv*, 2015.
- Kingma, D. P. and Ba, J. Adam: A method for stochastic optimization, 2014.
- Klein, A., Mazutis, L., Akartuna, I., Tallapragada, N., Veres, A., Li, V., Peshkin, L., Weitz, D., and Kirschner, M. Droplet barcoding for single-cell transcriptomics applied to embryonic stem cells. *Cell*, 161(5):1187–1201, 2015.
- Langford, J., Salakhutdinov, R., and Zhang, T. Learning nonlinear dynamic models. In *International Conference on Machine Learning*, pp. 593–600, 2009.
- Langley, P. Crafting papers on machine learning. In *International Conference on Machine Learning*, pp. 1207–1216, 2000.
- Li, W., Liu, S., Zha, H., and Zhou, H. Parametric fokker-planck equation. In *Geometry science of information*, 2019.
- Liu, Q. and Wang, D. Stein variational gradient descent: A general purpose bayesian inference algorithm. In *Neural Information Processing Systems*, pp. 2378–2386, 2016.
- Milstein, G. N. and Tretyakov, M. V. (eds.). *Stochastic numerics for mathematical physics*. Springer Science & Business Media, 2013.
- Miyato, T., Kataoka, T., Koyama, M., and Yoshida, Y. Spectral normalization for generative adversarial networks. *arXiv preprint arXiv:1802.05957*, 2018.
- Nelson, E. *Quantum fluctuations*. Princeton University Press, 1985.
- Pavon, M., Tabak, E. G., and Trigila, G. The data-driven schrodinger bridge. *arXiv preprint arXiv:1806.01364*, 2018.
- Qi, D. and Majda, A. Low-dimensional reduced-order models for statistical response and uncertainty quantification: Two-layer baroclinic turbulence. *Journal of the Atmospheric Sciences*, 73(12):4609–4639, 2016.
- Rezende, D. and Mohamed, S. Variational inference with normalizing flows. In *arXiv preprint arXiv:1505.05770*, 2015.
- Risken, H. The fokker-planck equation. *Springer Series in Synergetics*, 18:4609–4639, 1989.
- Villani, C. *Optimal transport: old and new*, volume 338. Springer Science & Business Media, 2008.
- Wang, Y., Dai, B., Kong, L., Erfani, S. M., Bailey, J., and Zha, H. Learning deep hidden nonlinear dynamics from aggregate data. In *Uncertainty in Artificial Intelligence*, 2018.
- Weinan, E., Han, J., and Jentzen, A. Deep learning-based numerical methods for high-dimensional parabolic partial differential equations and backward stochastic differential equations. In *Communications in Mathematics and Statistics*, pp. 349–380, 2017.
- Zang, Y., Bao, G., Ye, X., and Zhou, H. Weak adversarial networks for high-dimensional partial differential equations. In *arXiv preprint arXiv:1907.08272*, 2019.



## A. Proofs

### A.1. Proof of Theorem 1

**Lemma A.1.** Suppose  $\phi(x): \mathbb{R}^d \mapsto \mathbb{R}^n$  have a continuous partial time derivative and continuous second partial space derivatives, then the density of  $\phi$  that satisfies (1) leads to Fokker Planck Equation:

$$\frac{\partial P}{\partial t} = \sum_{i=1}^D -\frac{\partial}{\partial x_i} [g(x)P(x, t)] + \frac{1}{2}\sigma^2 \sum_{i,j=1}^D \frac{\partial^2}{\partial x_i \partial x_j} P(x, t)$$

*Proof.* This result has been widely proved, here we just give a simple sketch of proof. Suppose  $\phi(x, t)$  is a solution of (1), by Itô formula we have:

$$d\phi = \left( \frac{\partial \phi}{\partial t} + g \frac{\partial \phi}{\partial x} + \frac{1}{2}\sigma^2 \frac{\partial^2 \phi}{\partial x^2} \right) dt + \sigma \frac{\partial \phi}{\partial x} dW$$

Let  $\frac{\partial \phi}{\partial t} = 0$ , then we take expectation on both sides:

$$d\mathbb{E}[\phi] = \mathbb{E} \left[ g \frac{\partial \phi}{\partial x} + \frac{1}{2}\sigma^2 \frac{\partial^2 \phi}{\partial x^2} \right] dt$$

$$\int_X \phi \frac{\partial P}{\partial t} dx = \int_X g \frac{\partial \phi}{\partial x} P(x, t) dx + \int_X \frac{1}{2}\sigma^2 \frac{\partial^2 \phi}{\partial x^2} P(x, t) dx$$

Use integration by parts on right side and consider  $P(\infty, t) = 0$ , we have:

$$\int_X \phi \frac{\partial P}{\partial t} dx = - \int_X \phi \frac{\partial}{\partial x} [g(x)P(x, t)] dx + \int_X \frac{1}{2}\sigma^2 \phi \frac{\partial^2 P(x, t)}{\partial x^2} dx$$

Finally we have 1-dimensional form of Fokker Planck Equation:

$$\frac{\partial P}{\partial t} = -\frac{\partial}{\partial x} [g(x)P(x, t)] + \frac{1}{2}\sigma^2 \frac{\partial^2 P(x, t)}{\partial x^2}$$

We extend 1-dimensional form to multi-dimensional form to get proof done. □

**Theorem A.1.** Suppose  $f$  satisfies  $\|\nabla f\| \leq 1$  and generated data evolves only one step from  $x_{t_{m-1}}$  by (2), define an operator:

$$F(x_t) = \frac{1}{N} \sum_{k=1}^N \left( \sum_{i=1}^D g(x_t^{(k)}) \frac{\partial}{\partial x_i} f(x_t^{(k)}) + \frac{1}{2}\sigma^2 \sum_{i,j=1}^D \frac{\partial^2}{\partial x_i \partial x_j} f(x_t^{(k)}) \right) \quad (13)$$

then the weak form of Wasserstein distance between real data and generated data at time point  $t_m$  can be approximated by:

$$\max_{\|\nabla f\| \leq 1} \left( \frac{1}{N} \sum_{k=1}^N f(x_{t_m}^{(k)}) - \frac{1}{N} \sum_{k=1}^N f(x_{t_{m-1}}^{(k)}) - \frac{\Delta t}{2} [F(x_{t_{m-1}}) + F(x_{t_m})] \right) \quad (14)$$

*Proof.* Suppose  $x_{t_m}^{(k)}$  and  $x_{t_{m-1}}^{(k)}$  are our observed samples at  $t_m$  and  $t_{m-1}$  respectively, then expectations could be approximated by observed samples and generated data:

$$\mathbb{E}_{X \sim \hat{P}(x, t_m)} [f(X)] = \int_X f(x) \hat{P}(x, t_m) dx \approx \frac{1}{N} \sum_{k=1}^N f(x_{t_m}^{(k)}), \quad (15)$$

$$\begin{aligned}
 \mathbb{E}_{X \sim \tilde{P}(x, t_m)}[f(X)] &= \int_X f(x) \tilde{P}(x, t_m) dx = \int_X f(x) \left[ \hat{P}(x, t_{m-1}) + \int_{t_{m-1}}^{t_m} \frac{\partial P(x, \tau)}{\partial t} d\tau \right] dx \\
 &= \int_X f(x) \hat{P}(x, t_{m-1}) dx + \int_X f(x) \int_{t_{m-1}}^{t_m} \frac{\partial P(x, \tau)}{\partial t} d\tau dx \\
 &\approx \frac{1}{N} \sum_{k=1}^N f(x_{t_{m-1}}^{(k)}) + \underbrace{\int_X f(x) \int_{t_{m-1}}^{t_m} \left\{ - \sum_{i=1}^D \frac{\partial}{\partial x_i} [g(x)P(x, \tau)] + \frac{1}{2} \sigma^2 \sum_{i,j=1}^D \frac{\partial^2}{\partial x_i \partial x_j} P(x, \tau) \right\} d\tau dx}_I \quad (16)
 \end{aligned}$$

Then for the second term I above, it is difficult to calculate directly, but we can use integration by parts to rewrite I as:

$$\begin{aligned}
 I &= \int_{t_{m-1}}^{t_m} \int_X \left[ \sum_{i=1}^D -f(x) \frac{\partial}{\partial x_i} g(x) P(x, \tau) + \frac{1}{2} \sigma^2 \sum_{i,j=1}^D f(x) \frac{\partial^2}{\partial x_i \partial x_j} P(x, \tau) \right] dx d\tau \\
 &= \int_{t_{m-1}}^{t_m} \int_X \left[ \sum_{i=1}^D g(x) P(x, \tau) \frac{\partial}{\partial x_i} f(x) + \frac{1}{2} \sigma^2 \sum_{i,j=1}^D P(x, \tau) \frac{\partial^2}{\partial x_i \partial x_j} f(x) \right] dx d\tau \\
 &= \int_{t_{m-1}}^{t_m} \left( \mathbb{E}_{x \sim \tilde{P}(x, \tau)} \left[ \sum_{i=1}^D g(x) \frac{\partial}{\partial x_i} f(x) \right] + \mathbb{E}_{x \sim \tilde{P}(x, \tau)} \left[ \frac{1}{2} \sigma^2 \sum_{i,j=1}^D \frac{\partial^2}{\partial x_i \partial x_j} f(x) \right] \right) d\tau \\
 &= \int_{t_{m-1}}^{t_m} \frac{1}{N} \sum_{k=1}^N \left( \sum_{i=1}^D g(x^{(k)}) \frac{\partial}{\partial x_i} f(x^{(k)}) + \frac{1}{2} \sigma^2 \sum_{i,j=1}^D \frac{\partial^2}{\partial x_i \partial x_j} f(x^{(k)}) \right) d\tau \quad (17)
 \end{aligned}$$

To approximate the integral from  $t_{m-1}$  to  $t_m$ , we adopt an average method between two endpoints, then we could rewrite the expectation in Equation (16) as:

$$\begin{aligned}
 \mathbb{E}_{x \sim \tilde{P}(x, t_m)}[f(x)] &\approx \frac{1}{N} \sum_{k=1}^N f(x_{t_{m-1}}^{(k)}) + \frac{\Delta t}{2} \left[ \frac{1}{N} \sum_{k=1}^N \left( \sum_{i=1}^D g(x_{t_{m-1}}^{(k)}) \frac{\partial}{\partial x_i} f(x_{t_{m-1}}^{(k)}) + \frac{1}{2} \sigma^2 \sum_{i,j=1}^D \frac{\partial^2}{\partial x_i \partial x_j} f(x_{t_{m-1}}^{(k)}) \right) \right. \\
 &\quad \left. + \frac{1}{N} \sum_{k=1}^N \left( \sum_{i=1}^D g(x_{t_m}^{(k)}) \frac{\partial}{\partial x_i} f(x_{t_m}^{(k)}) + \frac{1}{2} \sigma^2 \sum_{i,j=1}^D \frac{\partial^2}{\partial x_i \partial x_j} f(x_{t_m}^{(k)}) \right) \right] \\
 &= \frac{1}{N} \sum_{k=1}^N f(x_{t_{m-1}}^{(k)}) + \frac{\Delta t}{2} [F(x_{t_{m-1}}) + F(x_{t_m})] \quad (18)
 \end{aligned}$$

Put (13), (15) and (18) together to finish the proof.  $\square$

## A.2. Proof of Theorem 2

**Theorem A.2.** Suppose  $f$  satisfies  $\|\nabla f\| \leq 1$  and generated data evolves multiple steps from any initial data  $x_{t_{m_0}}$  by (2), define the operator:

$$F(x_t) = \frac{1}{N} \sum_{k=1}^N \left( \sum_{i=1}^D g(x_t^{(k)}) \frac{\partial}{\partial x_i} f(x_t^{(k)}) + \frac{1}{2} \sigma^2 \sum_{i,j=1}^D \frac{\partial^2}{\partial x_i \partial x_j} f(x_t^{(k)}) \right)$$

then for arbitrary  $n$ , the weak form of Wasserstein distance between real data and generated data at time point  $t_{m_n}$  can be approximated by:

$$\max_{\|\nabla f\| \leq 1} \left\{ \frac{1}{N} \sum_{k=1}^N f(x_{t_{m_n}}^{(k)}) - \frac{1}{N} \sum_{k=1}^N f(x_{t_{m_0}}^{(k)}) - \frac{\Delta t}{2} \left( F(x_{t_{m_0}}) + F(x_{t_{m_n}}) + 2 \sum_{s=1}^{n-1} F(x_{t_{m_s}}) \right) \right\} \quad (19)$$

*Proof.* Given initial  $x_{t_{m_0}}$  and an updated  $g(x)$ , we generate  $x_{t_{m_1}}, x_{t_{m_2}}, x_{t_{m_3}} \dots x_{t_{m_n}}$  sequentially by (2). Then the expectations can be rewritten as:

$$\mathbb{E}_{X \sim \hat{P}(x, t_{m_n})}[f(X)] = \int_X f(x) \hat{P}(x, t_{m_n}) dx \approx \frac{1}{N} \sum_{k=1}^N f(x_{t_{m_n}}^{(k)}), \quad (20)$$

$$\begin{aligned} \mathbb{E}_{X \sim \tilde{P}(x, t_{m_n})}[f(x)] &\approx \frac{1}{N} \sum_{k=1}^N f(x_{t_{m_0}}^{(k)}) + \int_{t_{m_0}}^{t_{m_1}} \frac{1}{N} \sum_{k=1}^N \left[ \sum_{i=1}^D g(x^{(k)}) \frac{\partial}{\partial x_i} f(x^{(k)}) + \frac{1}{2} \sigma^2 \sum_{i,j=1}^D \frac{\partial^2}{\partial x_i \partial x_j} f(x^{(k)}) \right] d\tau \\ &+ \int_{t_{m_1}}^{t_{m_2}} \frac{1}{N} \sum_{k=1}^N \left[ \sum_{i=1}^D g(x^{(k)}) \frac{\partial}{\partial x_i} f(x^{(k)}) + \frac{1}{2} \sigma^2 \sum_{i,j=1}^D \frac{\partial^2}{\partial x_i \partial x_j} f(x^{(k)}) \right] d\tau + \dots \\ &+ \int_{t_{m_{n-1}}}^{t_{m_n}} \frac{1}{N} \sum_{k=1}^N \left[ \sum_{i=1}^D g(x^{(k)}) \frac{\partial}{\partial x_i} f(x^{(k)}) + \frac{1}{2} \sigma^2 \sum_{i,j=1}^D \frac{\partial^2}{\partial x_i \partial x_j} f(x^{(k)}) \right] d\tau \end{aligned} \quad (21)$$

which is:

$$\begin{aligned} \mathbb{E}_{X \sim \tilde{P}(X, t_{m_n})}[f(x)] &\approx \frac{1}{N} \sum_{k=1}^N f(x_{t_{m_0}}^{(k)}) + \frac{\Delta t}{2} \left[ \frac{1}{N} \sum_{k=1}^N \left( \sum_{i=1}^D g(x_{t_{m_0}}^{(k)}) \frac{\partial}{\partial x_i} f(x_{t_{m_0}}^{(k)}) + \frac{1}{2} \sigma^2 \sum_{i,j=1}^D \frac{\partial^2}{\partial x_i \partial x_j} f(x_{t_{m_0}}^{(k)}) \right) \right. \\ &+ \left. \frac{1}{N} \sum_{k=1}^N \left( \sum_{i=1}^D g(x_{t_{m_1}}^{(k)}) \frac{\partial}{\partial x_i} f(x_{t_{m_1}}^{(k)}) + \frac{1}{2} \sigma^2 \sum_{i,j=1}^D \frac{\partial^2}{\partial x_i \partial x_j} f(x_{t_{m_1}}^{(k)}) \right) \right] \\ &+ \frac{\Delta t}{2} \left[ \frac{1}{N} \sum_{k=1}^N \left( \sum_{i=1}^D g(x_{t_{m_1}}^{(k)}) \frac{\partial}{\partial x_i} f(x_{t_{m_1}}^{(k)}) + \frac{1}{2} \sigma^2 \sum_{i,j=1}^D \frac{\partial^2}{\partial x_i \partial x_j} f(x_{t_{m_1}}^{(k)}) \right) \right. \\ &+ \left. \frac{1}{N} \sum_{k=1}^N \left( \sum_{i=1}^D g(x_{t_{m_2}}^{(k)}) \frac{\partial}{\partial x_i} f(x_{t_{m_2}}^{(k)}) + \frac{1}{2} \sigma^2 \sum_{i,j=1}^D \frac{\partial^2}{\partial x_i \partial x_j} f(x_{t_{m_2}}^{(k)}) \right) \right] + \dots \\ &+ \frac{\Delta t}{2} \left[ \frac{1}{N} \sum_{k=1}^N \left( \sum_{i=1}^D g(x_{t_{m_{n-1}}}^{(k)}) \frac{\partial}{\partial x_i} f(x_{t_{m_{n-1}}}^{(k)}) + \frac{1}{2} \sigma^2 \sum_{i,j=1}^D \frac{\partial^2}{\partial x_i \partial x_j} f(x_{t_{m_{n-1}}}^{(k)}) \right) \right. \\ &+ \left. \frac{1}{N} \sum_{k=1}^N \left( \sum_{i=1}^D g(x_{t_{m_n}}^{(k)}) \frac{\partial}{\partial x_i} f(x_{t_{m_n}}^{(k)}) + \frac{1}{2} \sigma^2 \sum_{i,j=1}^D \frac{\partial^2}{\partial x_i \partial x_j} f(x_{t_{m_n}}^{(k)}) \right) \right] \\ &= \frac{1}{N} \sum_{k=1}^N f(x_{t_{m_0}}^{(k)}) + \frac{\Delta t}{2} \left\{ \frac{1}{N} \sum_{k=1}^N \left( \sum_{i=1}^D g(x_{t_{m_0}}^{(k)}) \frac{\partial}{\partial x_i} f(x_{t_{m_0}}^{(k)}) + \frac{1}{2} \sigma^2 \sum_{i,j=1}^D \frac{\partial^2}{\partial x_i \partial x_j} f(x_{t_{m_0}}^{(k)}) \right) \right. \\ &+ \frac{1}{N} \sum_{k=1}^N \left( \sum_{i=1}^D g(x_{t_{m_n}}^{(k)}) \frac{\partial}{\partial x_i} f(x_{t_{m_n}}^{(k)}) + \frac{1}{2} \sigma^2 \sum_{i,j=1}^D \frac{\partial^2}{\partial x_i \partial x_j} f(x_{t_{m_n}}^{(k)}) \right) \\ &+ \left. \left. 2 \sum_{s=1}^{n-1} \left[ \frac{1}{N} \sum_{k=1}^N \left( \sum_{i=1}^D g(x_{t_{m_s}}^{(k)}) \frac{\partial}{\partial x_i} f(x_{t_{m_s}}^{(k)}) + \frac{1}{2} \sigma^2 \sum_{i,j=1}^D \frac{\partial^2}{\partial x_i \partial x_j} f(x_{t_{m_s}}^{(k)}) \right) \right] \right\} \end{aligned} \quad (22)$$

Put (13), (20) and (22) together, finally it comes to:

$$\mathbb{E}_{X \sim \tilde{P}(X, t_{m_n})}[f(x)] \approx \frac{1}{N} \sum_{k=1}^N f(x_{t_{m_0}}^{(k)}) + \frac{\Delta t}{2} \left( F(x_{t_{m_0}}) + F(x_{t_{m_n}}) + 2 \sum_{s=1}^{n-1} F(x_{t_{m_s}}) \right) \quad (23)$$

□

### A.3. Proof of Theorem 3

**Theorem A.3.** Denote the mean of real data as  $x_{mean}$ , suppose the real data and fake data are both bounded by a boundary function  $b(x) = 0$ , then the distance between data point  $x_i$  and  $b(x) = 0$  is approximated by:

$$dis(x_i, b(x)) \approx (1 - y) \|x_i - x_{mean}\|_2 \quad (24)$$

where  $y$  is the solution of:

$$b(yx_i - yx_{mean}) = 0 \quad (25)$$

if we assume real data evolves inside of a bounded area, first we attempt to bound it with an elliptical area:

$$b(x) = \left\| \frac{x - x_{mean}}{\sigma} \right\|_2^2 - 1 = 0 \quad (26)$$

then we derive the value of  $y$  would be:

$$y = \sqrt{\frac{1}{\left\| \frac{proj_{\sigma} \mathbf{x}}{\sigma} \right\|_2^2}} \quad (27)$$

where  $proj_{\sigma} \mathbf{x}$  is the projection of  $(x_i - x_{mean})$  on principal component  $\sigma$  of the data.

*Proof.* By Singular Value Decomposition, we know singular value  $\sigma$  and principal component vector  $v$ , then the projection of  $(x_i - x_{mean})$  on  $d_{th}$  principal component can be written as:

$$(x_i - x_{mean}) \cdot v_d = proj_{\sigma_d} \mathbf{x} \quad (28)$$

$$(x_i - x_{mean}) = proj_{\sigma_d} \mathbf{x} \cdot v_d \quad (29)$$

Consider  $x_i - x_{mean}$  intersects  $b(x) = 0$  at  $x'_i$ , then we have:

$$x'_i - x_{mean} = y(x_i - x_{mean}) \quad (30)$$

Plug  $x'_i - x_{mean}$  into  $b(x) = 0$  we have:

$$\sum_{d=1}^D \left| \frac{x'_i - x_{mean}}{\sigma_d} \right|^2 = \sum_{d=1}^D \left| y \frac{proj_{\sigma_d} \mathbf{x}}{\sigma_d} \right|^2 = \left\| y \frac{proj_{\sigma} \mathbf{x}}{\sigma} \right\|_2^2 = 1 \quad (31)$$

Finally the value of  $y$  and the distance will be:

$$y = \sqrt{\frac{1}{\left\| \frac{proj_{\sigma} \mathbf{x}}{\sigma} \right\|_2^2}} \quad (32)$$

$$dis(x_i, b(x)) \approx \|x_i - x'_i\| = (1 - y) \|(x_i - x_{mean})\|_2 \quad (33)$$

□

#### A.4. Proof of Theorem 4

Suppose ground truth of drift function in Euler form is  $g_r(x)$ , approximated drift function learned from data is  $g_f(x)$ , then original Itô process, the Euler evolve process and approximated evolve process are as follows:

$$dX = g(x)dt + \sigma dW \quad (34)$$

$$X_{t+\Delta t}^r = X_t^r + g_r(X_t^r)\Delta t + \sigma \sqrt{\Delta t}N^r(0, 1) \quad (35)$$

$$X_{t+\Delta t}^f = X_t^f + g_f(X_t^f)\Delta t + \sigma \sqrt{\Delta t}N^f(0, 1) \quad (36)$$

**Lemma A.2.** *With the same initial  $X_{t_0}$ , if there is a global Lipschitz constant  $K$  which satisfies:*

$$|g(x, t) - g(y, t)| \leq K|x - y| \quad (37)$$

*then after  $n$  steps, the expectation error between Itô process  $X_{t_n}$  and Euler forward process  $X_{t_n}^r$  is:*

$$\mathbb{E}|X_{t_n} - X_{t_n}^r| \leq K(1 + E|X_0|^2)^{1/2} \Delta t \quad (38)$$

*Proof.* The proof process is quite long and out of the scope of this paper, for more details please see first two chapters in reference book (Milstein & Tretyakov, 2013).  $\square$

**Theorem A.4.** *With the same initial  $X_{t_0}$ , suppose the generalization error of neural network  $g(x)$  is  $\varepsilon$ , for some global Lipschitz constant  $K$ :*

$$|g(x) - g(y)| \leq K|x - y| \quad (39)$$

*the derivative of  $g(x)$  satisfies:*

$$\sup g'(x) = L \quad (40)$$

*then after  $n$  steps with step size  $\Delta t = T/n$ , the expectation error between Itô process  $X_{t_n}$  and approximated forward process  $X_{t_n}^f$  is bounded by:*

$$\mathbb{E}|X_{t_n} - X_{t_n}^f| \leq \frac{\varepsilon}{L}(e^{LT} - 1) + K(1 + E|X_0|^2)^{1/2} \Delta t \quad (41)$$

*Proof.* For initial  $X$  and first one-step iteration:

$$\begin{cases} X_{t_0}^r = X_{t_0} \\ X_{t_0}^f = X_{t_0} \end{cases} \quad (42)$$

$$\begin{cases} X_{t_1}^r = X_{t_0}^r + g_r(X_{t_0}^r)\Delta t + \sigma \sqrt{\Delta t}N^r(0, 1) \\ X_{t_1}^f = X_{t_0}^f + g_f(X_{t_0}^f)\Delta t + \sigma \sqrt{\Delta t}N^f(0, 1) \end{cases} \quad (43)$$

Then we have:

$$\mathbb{E}|X_{t_0}^r - X_{t_0}^f| = \mathbb{E}|X_{t_0} - X_{t_0}| = 0 \quad (44)$$

$$\begin{aligned} \mathbb{E}|X_{t_1}^r - X_{t_1}^f| &= \mathbb{E}|X_{t_0}^r - X_{t_0}^f + g_r(X_{t_0}^r)\Delta t - g_f(X_{t_0}^f)\Delta t + \sigma \sqrt{\Delta t}N^r(0, 1) - \sigma \sqrt{\Delta t}N^f(0, 1)| \\ &\leq \mathbb{E}|X_{t_0}^r - X_{t_0}^f| + \mathbb{E}|g_r(X_{t_0}^r) - g_f(X_{t_0}^f)|\Delta t \\ &= \mathbb{E}|g_r(X_{t_0}^r) - g_f(X_{t_0}^r) + g_f(X_{t_0}^r) - g_f(X_{t_0}^f)|\Delta t \\ &\leq \mathbb{E}|g_r(X_{t_0}^r) - g_f(X_{t_0}^r)|\Delta t + \mathbb{E}|g_f(X_{t_0}^r) - g_f(X_{t_0}^f)|\Delta t \\ &\leq \varepsilon\Delta t + \mathbb{E}|g_f(X_{t_0}^r) - g_f(X_{t_0}^f)|\Delta t \\ &= \varepsilon\Delta t + \mathbb{E}|g_f'(X_{t_0}^\xi)(X_{t_0}^r - X_{t_0}^f)|\Delta t \quad (X_{t_0}^\xi \in [X_{t_0}^r, X_{t_0}^f]) \\ &\leq \varepsilon\Delta t + L\mathbb{E}|X_{t_0}^r - X_{t_0}^f|\Delta t \\ &= \varepsilon\Delta t \end{aligned} \quad (45)$$

Follow the pattern of (45) we have:

$$\begin{cases} X_{t_2}^r = X_{t_1}^r + g_r(X_{t_1}^r)\Delta t + \sigma\sqrt{\Delta t}N^r(0, 1) \\ X_{t_2}^f = X_{t_1}^f + g_f(X_{t_1}^f)\Delta t + \sigma\sqrt{\Delta t}N^f(0, 1) \end{cases} \quad (46)$$

...

$$\begin{cases} X_{t_n}^r = X_{t_{n-1}}^r + g_r(X_{t_{n-1}}^r)\Delta t + \sigma\sqrt{\Delta t}N^r(0, 1) \\ X_{t_n}^f = X_{t_{n-1}}^f + g_f(X_{t_{n-1}}^f)\Delta t + \sigma\sqrt{\Delta t}N^f(0, 1) \end{cases} \quad (47)$$

Which leads to:

$$\begin{aligned} \mathbb{E}|X_{t_2}^r - X_{t_2}^f| &= \mathbb{E}|X_{t_1}^r - X_{t_1}^f + g_r(X_{t_1}^r)\Delta t - g_f(X_{t_1}^f)\Delta t + \sigma\sqrt{\Delta t}N^r(0, 1) - \sigma\sqrt{\Delta t}N^f(0, 1)| \\ &\leq \mathbb{E}|X_{t_1}^r - X_{t_1}^f| + \mathbb{E}|g_r(X_{t_1}^r) - g_f(X_{t_1}^f)|\Delta t \\ &\leq \mathbb{E}|X_{t_1}^r - X_{t_1}^f| + \varepsilon\Delta t + L\mathbb{E}|X_{t_1}^r - X_{t_1}^f|\Delta t \\ &\leq (1 + L\Delta t)\varepsilon\Delta t + \varepsilon\Delta t \end{aligned} \quad (48)$$

...

$$\mathbb{E}|X_{t_n}^r - X_{t_n}^f| \leq \varepsilon\Delta t \sum_{i=0}^{n-1} (1 + L\Delta t)^i \quad (49)$$

Now let  $S = \sum_{i=0}^{n-1} (1 + L\Delta t)^i$ , then consider followings:

$$\begin{aligned} S(L\Delta t) &= S(1 + L\Delta t) - S \\ &= \sum_{i=1}^n (1 + L\Delta t)^i - \sum_{i=0}^{n-1} (1 + L\Delta t)^i \\ &= (1 + L\Delta t)^n - 1 \\ &= \left(1 + L\frac{T}{n}\right)^n - 1 \\ &\leq e^{LT} - 1 \end{aligned} \quad (50)$$

Finally we have:

$$\mathbb{E}|X_{t_n}^r - X_{t_n}^f| \leq \frac{\varepsilon}{L}(e^{LT} - 1) \quad (51)$$

Combining with (38) gives:

$$\mathbb{E}|X_{t_n}^r - X_{t_n}^f| \leq \frac{\varepsilon}{L}(e^{LT} - 1) + K(1 + E|X_0|^2)^{1/2}\Delta t \quad (52)$$

□